Effects of El Niño–Southern Oscillation on the Climate, Water Balance, and Streamflow of the Mississippi River Basin

TRACY E. TWINE

Department of Atmospheric Sciences, University of Illinois at Urbana–Champaign, Urbana, Illinois

CHRISTOPHER J. KUCHARIK AND JONATHAN A. FOLEY

Center for Sustainability and the Global Environment, University of Wisconsin—Madison, Madison, Wisconsin

(Manuscript received 29 March 2004, in final form 3 June 2005)

ABSTRACT

Climatic and hydrologic observations and results from a terrestrial ecosystem model coupled to a regional-scale river-routing algorithm are used to document the associations between the El Niño–Southern Oscillation (ENSO) phenomenon and anomalies in climate, surface water balance, and river hydrology within the Mississippi River basin. While no ENSO signal is found in streamflow at the outlet of the basin in Vicksburg, Mississippi, significant anomalies in all water balance components are found in certain regions within the basin. ENSO is mainly associated with positive winter temperature anomalies, but hydrologic patterns vary with season, location, and ENSO phase. El Niño precipitation anomalies tend to affect evapotranspiration (ET) in the western half of the basin and runoff in the eastern half. La Niña events are associated with ET anomalies in the central portion of the basin and runoff anomalies in the southern and eastern portions of the basin. Both ENSO phases are associated with decreased snow depth. Anomalous soil moisture patterns occur at seasonal time scales and filter noisier spatial patterns of precipitation anomalies into coherent patterns with larger field significance; however, for all water budget components, there is a large amount of variability in response within a particular ENSO phase. With anomalies that are up to 4 times those of a typical event, it is clear that improved predictability of the onset and strength of an upcoming ENSO event is important for both water resource management and disaster mitigation.

1. Introduction

The Mississippi River basin covers roughly 3.2 million km^2 and is home to a $100 billion per year agricultural economy (Goolsby et al. 1999). Given the importance of this basin in terms of environmental processes, natural resources, and economics, it is important to understand how these factors may be affected by climate variability. The Global Energy and Water Cycle Experiment (GEWEX) Continental-Scale International Project (GCIP) quantified the energy and water cycles within the basin using observational analyses and model intercomparison (Berbery et al. 2003; Betts et al. 2003; Roads et al. 2003). The GCIP effort was able to provide a measure of uncertainty in the estimates of water budget components (Roads et al. 2003) and the motivation for an examination of the uncertainty in long-lead-time predictability of the water cycle. The mission of a new effort, GEWEX Americas Prediction Project (GAPP), is to demonstrate skill in predicting changes in water resources on time scales up to seasonal and annual (Robock 2003).

One of the most studied patterns of the world's climate that acts at a seasonal to annual time scale is the El Niño–Southern Oscillation (ENSO) phenomenon. The ENSO warm phase (El Niño) and cold phase (La Niña) have both been linked to anomalous climatic patterns in parts of the Mississippi River basin (Gershunov and Barnett 1998; Montroy et al. 1998; Ropelewski and Halpert 1986; Smith et al. 1998), but few studies have investigated the role of ENSO on the individual terms of the surface water balance. Instead, previous studies have looked at more direct ties between ENSO and the

Corresponding author address: Tracy E. Twine, Department of Atmospheric Sciences, University of Illinois at Urbana–Champaign, 105 South Gregory Street, Urbana, IL 61801-3070.
E-mail: twine@atmos.uiuc.edu

climate and hydrology of this region. For example, Kunkel and Angel (1999) examined snowfall changes across the continental United States and found a spatially coherent pattern of decreased snowfall during El Niño and La Niña winters throughout much of the central Midwest, and a small area of increased snowfall over northern Wisconsin and Minnesota.

Other studies have considered the statistical correlation between ENSO and runoff or streamflow. Kahya and Dracup (1993) and Dracup and Kahya (1994) investigated patterns of streamflow in relation to El Niño and La Niña across the United States and determined that both El Niño and La Niña are correlated with changes in streamflow within specific regions. They associated below-normal seasonal streamflow with La Niña and above-normal seasonal streamflow with El Niño. Guetter and Georgakakos (1996) found statistically significant seasonal streamflow responses to El Niño and La Niña in the Iowa River basin (a basin draining an area of 8470 km^2 contained within the Mississippi River basin in eastern Iowa) using gauged streamflow data for the period 1904–89. They found correlations between the onset of El Niño conditions and a lagged increase in streamflow, and the onset of La Niña conditions and a lagged decrease in streamflow. Using a terrestrial hydrologic model with climate data for the period 1979–93, Chen and Kumar (2002) correlated positive anomalies of simulated runoff with El Niño events and negative anomalies with La Niña events.

In this study, we extrapolate the ENSO association to variables for which we have few observations across the basin. We first determine how simulated results of snow depth, soil moisture, and streamflow compare with observations and results of previous studies. We assume that if our simulations compare favorably, then we may reasonably represent the ENSO response to other simulated variables such as evapotranspiration (ET), total runoff (the sum of surface runoff and subsurface drainage), and snow depth and soil moisture for larger regions outside the domain of observations.

The methods for most of the streamflow studies listed above assume a linear ENSO response—El Niño and La Niña are assumed to be associated with opposite anomalies of climate, energy, and water budget components. Recent analyses of associations between climate anomalies and ENSO have found that the assumption of linearity may be incorrect (Mason and Goddard 2001; Montroy et al. 1998; and references therein). In this study, our methods do not assume a linear ENSO response. We separately evaluate the association between El Niño and La Niña events and the climate, surface water balance, and streamflow of the Mississippi River basin through a comprehensive analysis of ET, soil moisture, snow depth, total runoff, and streamflow anomalies. We use a combination of 1) climatic and hydrologic observations (including measurements of precipitation, temperature, soil moisture, snow cover, and streamflow) within the period 1958–2000; and 2) the results of a land surface/terrestrial ecosystem model, the Integrated Biosphere Simulator (IBIS; Foley et al. 1996; Kucharik 2003; Kucharik et al. 2000) coupled to a regional-scale river-routing algorithm, the Hydrological Routing Algorithm (HYDRA; Coe 2000). We use this combination of observations and model simulations to illustrate the connections between ENSO and changes in climate, surface water balance, and river hydrology, and to examine how they are distributed across the Mississippi River basin in time and space.

In section 2 we describe the observations and models used in the analysis. We examine the associations between El Niño and La Niña events with temperature and precipitation in section 3. In section 4 we evaluate our simulation results with observations of soil moisture, snow depth, and streamflow. We analyze IBIS–HYDRA results as they relate to ENSO in section 5, and in section 6 we discuss the variability in hydrologic response between weak and strong ENSO events.

2. Methods: Synthesis of models and observations

To determine how El Niño and La Niña events are related to changes in the surface water balance and streamflow of the Mississippi River basin (Fig. 1), we use available observations augmented with the results of model simulations for the 43-yr period of 1958–2000. We analyze monthly precipitation and temperature observations from the Climate Research Unit (CRU05) climate dataset (New et al. 1999, 2000) that includes gridded values derived from station observations, and monthly streamflow observations from the U.S. Geological Survey (USGS) at each subbasin outlet (http://water.usgs.gov/). There are insufficient observations to adequately quantify the intermediate reservoirs and fluxes involved within the water cycle, such as infiltration and soil moisture, snow depth, transpiration, evaporation from the soil surface and vegetation canopies, and surface runoff and subsurface drainage (Roads et al. 2003). We use IBIS and HYDRA to simulate variables with insufficient observational coverage, along with available observations of precipitation, temperature, streamflow, snow depth, and soil moisture to determine the relationship between ENSO and the Mississippi River basin water balance.

For both observations and simulated results, we bin

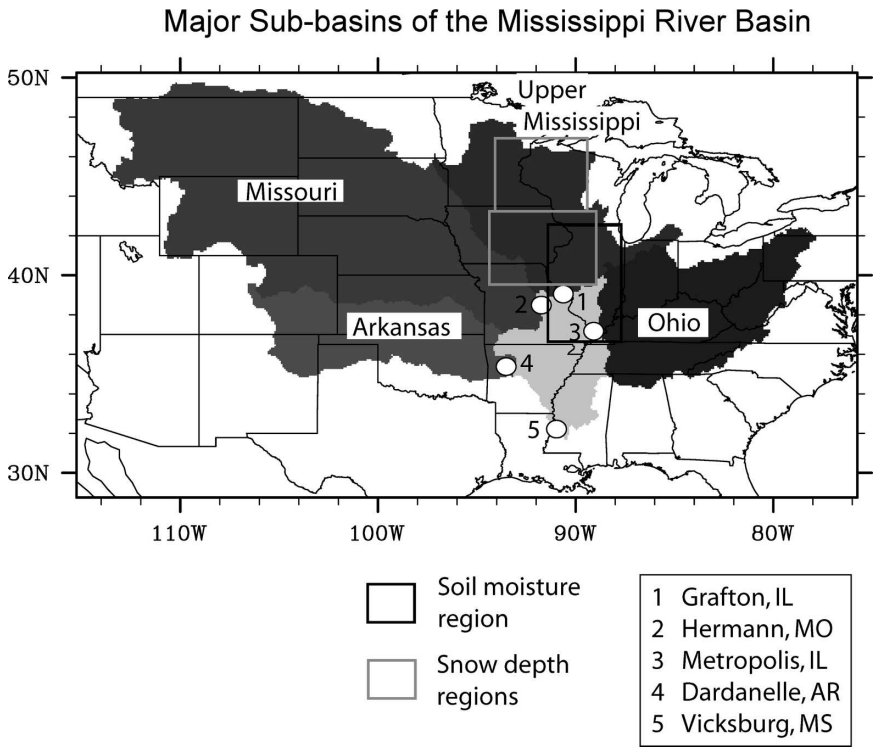

FIG. 1. Major subbasins of the Mississippi River basin: the Upper Mississippi with outlet at 1) Grafton, IL; the Missouri with outlet near 2) Hermann, MO; the Ohio with outlet at 3) Metropolis, IL; the Arkansas with outlet at 4) Dardanelle, AR; and the entire Mississippi with outlet at 5) Vicksburg, MS.

monthly values of each variable into an El Niño, La Niña, or neutral month category (Table 1), as presented in Trenberth (1997) for 1958–95 and as classified by the Climate Prediction Center for 1996–2000. The values of each bin are then grouped by season and used to determine seasonal averages. For example, values from all El Niño December months are grouped with those from all El Niño January and February months and averaged to create a winter [December–February (DJF)] El Niño average value. The average value of a "neutral season" is then subtracted from the average value of an "El Niño season" to determine the El Niño–related change in the variable. An identical procedure is used for the La Niña analysis. The binning of values from individual months into one of the three categories allows the El Niño–related anomaly and La Niña–related anomaly to be independent of each other, with no assumption of linearity in response. We use the anomaly from the neutral mean in order to be consistent with definitions from Trenberth (1997) and the Climate Prediction Center. We are not attempting to evaluate the predictability of water resources as a result of an ENSO event (Guetter and Georgakakos 1996; Maurer and Lettenmaier 2003), but we are attempting to quantify the change in particular water budget components during an average ENSO event. The Student's *t* test is used to evaluate the statistical significance of the anomalies.

a. Observations

1) CLIMATE

Because changes in the water balance, snow depth, and streamflow are forced by changes in regional climate, we use the monthly temperature and precipitation observations from 1958 to 2000, as reported in the CRU05 climate dataset (New et al. 1999, 2000) to present a summary of the ENSO-related changes in regional climate across the Mississippi River basin. The CRU05 dataset contains monthly values of climate variables interpolated to a 0.5° latitude × 0.5° longitude grid for the period 1901–2000. We analyze observations for the period 1958–2000 to coincide with the time period of the IBIS simulations described in section 2b. Observations from 1958–95 are analyzed from the original CRU05 time series (TS)1.0 dataset (New et al. 1999,

TABLE 1. Months (denoted by their first letter) corresponding to El Niño (black), La Niña (gray), and neutral (white) events according to Trenberth (1997) for 1958–95, and the Climate Prediction Center sea surface temperature analysis for 1996–2000.

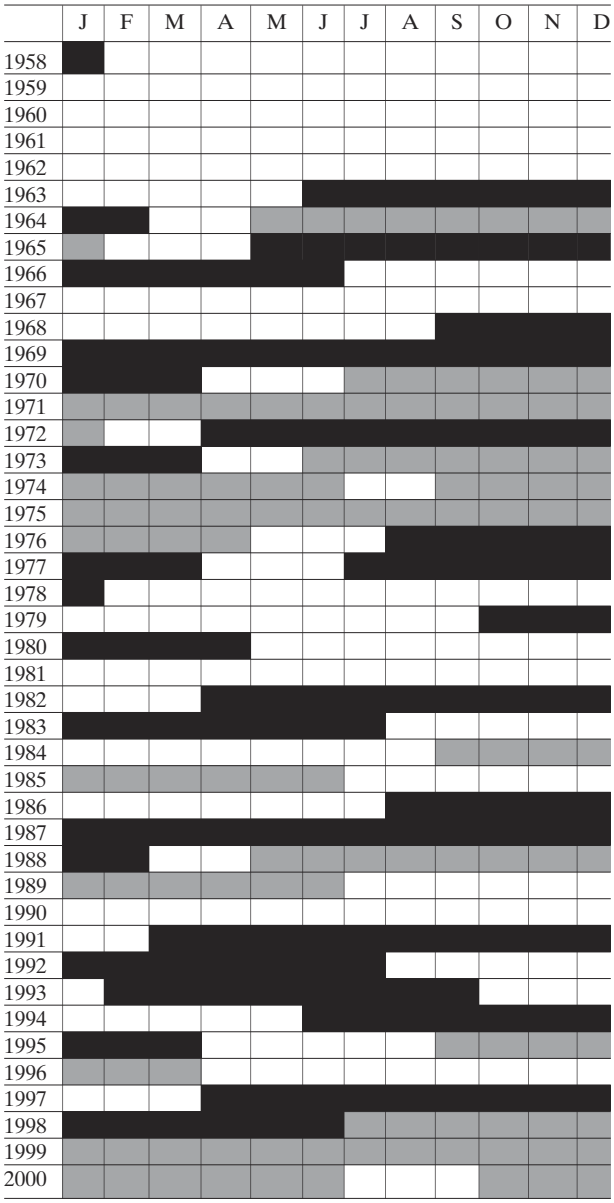

2000) because this dataset is used to drive the IBIS model for 1958–95. Observations from the revised TS2.0 (1901–2000) dataset are used from 1996 to 2000 because this dataset is used to drive the IBIS model for 1996–2000.

2) SOIL MOISTURE

Soil moisture measurements from 19 observation stations in Illinois are available from the Illinois Soil Moisture Network (Hollinger and Isard 1994). We use an average monthly value for Illinois that is the average of 16 stations over the 13-yr period of 1983–95 as presented in Lenters et al. (2000). Although these measurements were made over managed grass cover that does not match the land cover simulated by the model [see section 2b(1) below], we compare these available measurements with simulated results because this is the only dataset of soil moisture over a region contained within the Mississippi basin.

3) SNOW COVER

We analyze snow depth measurements from the National Weather Service (NWS) Summary of the Day dataset (http://www.ncdc.noaa.gov/onlineprod/tfsod/climvis/main.html) for the 192-month winter period of November–April 1963–95, as presented in Lenters et al. (2000). Data from 34 stations were analyzed in the Lenters et al. study and averaged over four quadrants of the north-central United States. Approximately half of these stations are located outside the Mississippi River basin; therefore, we analyze the 16 stations contained within the northwest and southwest quadrants of the Lenters et al. analysis. All of the stations within the southwest quadrant of the Lenters et al. analysis and five of the seven stations within the northwest quadrant are located within the Mississippi River basin. In this analysis we refer to the northwest quadrant of the Lenters et al. study as the northern region and the southwest quadrant as the southern region. The two quadrants containing the observation stations are shown in Fig. 1.

4) STREAMFLOW

For our analyses of the water budget and streamflow, we split the basin into four major subbasins: 1) the Upper Mississippi, with outlet to the Mississippi River at Grafton, Illinois; 2) the Ohio, with outlet to the Mississippi River at Metropolis, Illinois; 3) the Missouri, upstream of the confluence with the Mississippi at Hermann, Missouri; and 4) the Arkansas, upstream of the confluence with the Mississippi at Dardanelle, Arkansas (Fig. 1). These particular locations coincide with USGS stream gauge sites. We obtained annual and monthly average streamflow measurements from the USGS (http://waterdata.usgs.gov/nwis/sw) for the period 1958–2000 at Grafton, Illinois (site ID: 05587450); Hermann, Missouri (06934500); and Metropolis, Illinois (03611500). Data for the period 1958 through September 1994 were obtained at Dardanelle, Arkansas (07258000), and for the period 1958–98 at Vicksburg, Mississippi (07289000).

b. Model simulations

We use a regional version of IBIS, developed specifically for the Mississippi River basin (Twine et al. 2004), to simulate the water balance (including ET, soil moisture, snow depth, and surface runoff and subsurface drainage) and pass these results to a regional version of HYDRA, specifically developed and tested for the Mississippi River basin (Donner et al. 2002), to simulate streamflow.

1) IBIS LAND SURFACE/TERRESTRIAL ECOSYSTEM MODEL

IBIS is a regional- to global-scale terrestrial ecosystem model that includes modules for vegetation canopy physics, soil physics and hydrology, vegetation phenology, and ecosystem biogeochemistry. Much of the land surface module structure has been borrowed from the land surface transfer scheme (LSX) package (Thompson and Pollard 1995a,b). Each IBIS grid cell represents vegetation in two canopies: an upper-level forest canopy and a lower level of shrubs, cool (C3) and warm (C4) grasses, and crops. The model also includes 3 snow layers and 11 soil layers. The global version of IBIS has been tested and validated against surface flux observations (Delire and Foley 1999), biogeochemical observations (Kucharik et al. 2001), and global compilations of ecosystem and hydrological data (Foley et al. 1996; Kucharik et al. 2000). In a previous study, the global version of IBIS was adapted for use over the Mississippi River basin (Kucharik 2003; Twine et al. 2004).

IBIS requires climatic forcing for each model time step (1 h) on a 0.5° latitude × 0.5° longitude grid. We synthesize hourly weather and climate information from a combination of monthly climatic observations and daily reanalyzed meteorological data. We used observed monthly values of air temperature, precipitation, vapor pressure, and cloud fraction from 1901 to 1994 along with 1961–90 climatological mean values of monthly wind speed, diurnal temperature range, and number of wet days per month as given by the CRU05 climate dataset (New et al. 1999, 2000) to drive the model simulation through 1994. Recently, the Climate Research Unit reprocessed the climate dataset and attached subsequent data through 2000. We continued the IBIS run through December 2000 in order to include the most recent strong El Niño (1997/98), and La Niña (1998–2000) events, but we did not rerun the entire simulation with the new dataset.

To capture the transient, day-to-day phenomena of storm systems characteristic of the continental United States and to simulate spatial patterns of weather events, we combine the monthly CRU05 data with daily anomalies of temperature, precipitation, specific humidity, and cloud fraction from the National Centers for Environmental Prediction–National Center for Atmospheric Research (NCEP–NCAR) meteorological reanalysis dataset (Kalnay et al. 1996; Kistler et al. 2001) to produce a daily value at each grid cell. The monthly average values of these daily values are forced to equal the monthly CRU05 values. Hourly variations in climatic variables are simulated through the use of empirical formulations that relate temperature, specific humidity, precipitation, and radiation variability (Campbell and Norman 1998).

Although trends in the climate datasets may occur as a result of local, regional, or global climate change over the time period of this study, we did not detrend the data to eliminate this or other anomalous climate patterns that may influence surface water budget anomalies. This may skew our results toward greater or lesser effects of ENSO with time; however, we need to force the model with observed climate in order to validate our results with observations of surface water budget components such as soil moisture, snowfall, and streamflow.

The vegetation cover used in the simulation consists of a combination of potential vegetation cover (vegetation that could grow in a region without human intervention), and the fraction of corn, soybean, spring wheat, and winter wheat grown in the basin in 1992 (Fig. 2). The potential vegetation cover dataset was developed by Ramankutty and Foley (1998) and the crop cover dataset was developed by Donner (2003) by combining 1992 county-level U.S. agricultural inventory data for individual crops with the fractional cropland data of Ramankutty and Foley (1999). We use soil texture information from the conterminous United States (CONUS) dataset (Miller and White 1998) for each of the 11 soil layers. We neglect from our analysis the small area in Canada that is contained in the Mississippi basin as high-resolution crop cover data and soil texture information are not available for this area.

2) HYDRA LARGE-SCALE HYDROLOGICAL TRANSPORT ALGORITHM

HYDRA is a hydrological transport model that simulates the flow of water through streams, rivers, lakes, and wetlands in large watersheds (Coe 2000; Donner et al. 2002). The model uses topography, river flow directions, surface runoff, and subsurface drainage from the surrounding land areas to simulate the movement of water on a 5-min latitude/longitude grid.

River transport directions are specified with a multistep process from a combination of a digital elevation model (DEM), numerical correction techniques, and

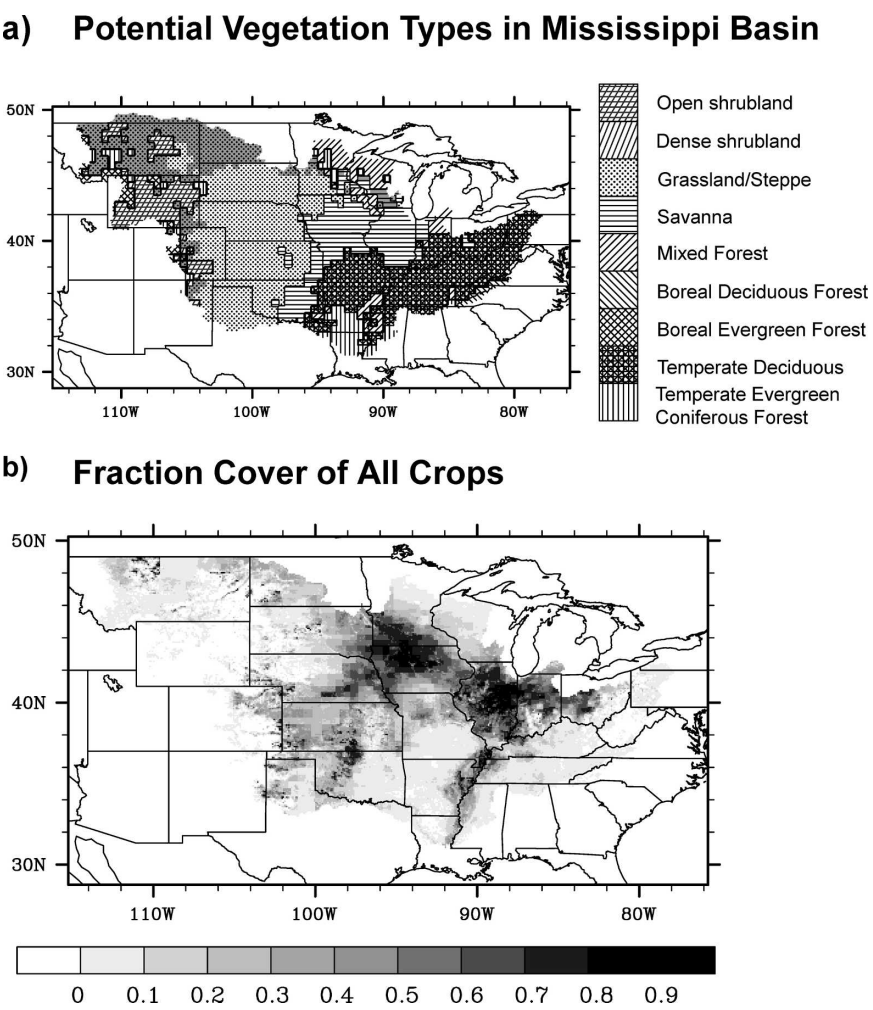

FIG. 2. (a) Potential vegetation cover of the Mississippi River basin. The gray-shaded area represents grasslands and savannas that are dominated by C3 grasses. Unshaded areas are dominated by mixtures of C4 grasses and C3 grasses. (b) 1992 total fraction cover of corn, soybean, spring wheat, and winter wheat as compiled by Donner (2003) from county-level census data and satellite information of crop cover.

subjective corrections. The total water entering each grid cell is the sum of local land surface runoff, local subsurface drainage and the flux of water into the grid cell from upstream. In this study, we do not account for dams and reservoirs or anthropogenic control (diversion of water) that may affect water resources mainly in the western portion of the Mississippi River basin. We also do not account for the flow through natural lakes or wetlands as they play a relatively minor role in the flow of water through the basin.

3) LINKING IBIS AND HYDRA

IBIS and HYDRA are used in sequence in our simulations. The IBIS model is first run using input climate, soils, and potential vegetation and crop cover information to simulate ET, soil moisture, snow depth, surface runoff, and subsurface drainage. Then the IBIS-simulated surface runoff and subsurface drainage are used as input to HYDRA where the water is routed through the river network to the basin outlet in Vicksburg, Mississippi.

For our simulations, we consider the entire Mississippi River basin, which falls within the region between 29° and 50°N and 115° and 78°W (Fig. 1). IBIS is run over this region at a 0.5° grid cell spatial resolution with an hourly time step for the period 1958–2000, after a model spinup period of over 100 yr that allows the soil biogeochemistry calculations of the model to nearly reach equilibrium. HYDRA then simulates streamflow

at rivers throughout the basin at a 5-min spatial resolution for the same 43-yr period, after a spinup period of 4 yr to allow the model reservoirs to nearly reach equilibrium.

To compare simulated soil moisture values with observations from the Illinois Soil Moisture Network, we average monthly values of simulated soil moisture over the region between 37° and 42.5°N and 91° and 88°W that comprises the network stations (Fig. 1). We also average monthly values of snow depth over the region between 43.5° and 47.5°N and 93.5° and 89.5°W to compare with the average snow depth observations from the seven stations contained within this northern region, and between 39.5° and 43.5°N and 94° and 89°W to compare with the average snow depth observations from the nine stations contained within this southern region (Fig. 1).

Previous versions of the combined IBIS–HYDRA modeling system have been tested over the Lake Chad region of Africa (Coe and Foley 2001), the Amazon River basin (Coe et al. 2002; Costa and Foley 1997; Foley et al. 2002), and the Mississippi River basin (Donner 2003; Donner and Kucharik 2003; Donner et al. 2002; Kucharik et al. 2001; Lenters et al. 2000). In a previous study (T. E. Twine et al. 2004; unpublished manuscript) it was determined that the IBIS–HYDRA modeling system correctly describes the major seasonal and interannual features of the terrestrial hydrology within the Mississippi River basin. The magnitudes of annual streamflow and interannual variability were well captured for the Upper Mississippi River and the entire Mississippi River. The annual average flow from the Ohio was underestimated by almost 30%, but the interannual variability was well simulated. At the seasonal time scale, the IBIS–HYDRA simulations showed a slight late bias in the spring peak of 1 month for all three subbasins. Simulated streamflow was not evaluated with observations from the Missouri and Arkansas subbasins as water flow is highly regulated. IBIS–HYDRA streamflow from the Missouri is especially overestimated because it is a large basin and contains many reservoirs and diversions of natural water flow for human consumption, irrigation, and industry. IBIS–HYDRA is physically based, and our goal is not to "tune" the model to any particular basin to simulate human management, but to better understand the natural cycling of water.

The underestimation of Ohio River streamflow is not uncommon in land surface models. An intercomparison of land surface process models revealed differences among models at the regional scale by up to a factor of 4 times the annual runoff (Lohmann et al. 2004). All of the major subbasins of the Mississippi River basin are large and drain areas with considerable diversity in terrain, climate, vegetation, and soil, but the Ohio basin also has a large transition from croplands in the north to mountains and forests in the south. Some combination of uncertainty in precipitation forcing, radiative forcing, canopy processes, and soil processes within the model combine to affect the simulated streamflow. While we continue to assess the accuracy of streamflow simulation and prediction, we can illuminate patterns in water budget components that are associated with an ENSO event because we reasonably represent the seasonal and interannual variability of streamflow.

3. ENSO and changes in regional climate

El Niño and La Niña events are associated with different temperature anomalies in the Mississippi River basin throughout the year, but both have the strongest link to temperature change in winter (Fig. 3). According to the CRU05 dataset, positive temperature anomalies occur throughout much of the basin during El Niño winters with the largest increases (2°C) in the Northern Plains and upper Midwest. These anomalies weaken drastically in spring when negative anomalies are found in the Arkansas River basin region. Negative anomalies of up to 1.5°C occur throughout much of the Missouri River basin in summer.

La Niña is also associated with positive temperature anomalies of 2°C during winter, but these anomalies are found mainly in the eastern half and southern tier of the basin (Fig. 3). The temperature anomalies shrink in area and weaken in spring. Negative anomalies are found throughout much of the Missouri River basin in fall (up to 1°C), but these anomalies are not significant at $p < 0.10$.

Precipitation patterns show that El Niño and La Niña are related to anomalies that are spatially and seasonally variable. During El Niño events, areas of negative precipitation anomalies of up to 1 mm day^{-1} are scattered throughout the eastern and southern portions of the basin in winter, spring, and summer, while positive precipitation anomalies of up to 1 mm day^{-1} are found in the northwestern region in summer and the Central Plains in summer and fall (Fig. 4). These areas of positive anomalies in the central region that begin in winter in the south and move northward throughout the year are consistent with similar patterns described by Ropelewski and Halpert (1986).

La Niña is linked to different, but not opposite, variations in precipitation. Areas of positive precipitation anomalies (about 1 mm day^{-1}) in the central and eastern portions of the basin in winter become negative in the spring (Fig. 4). These negative anomalies disperse

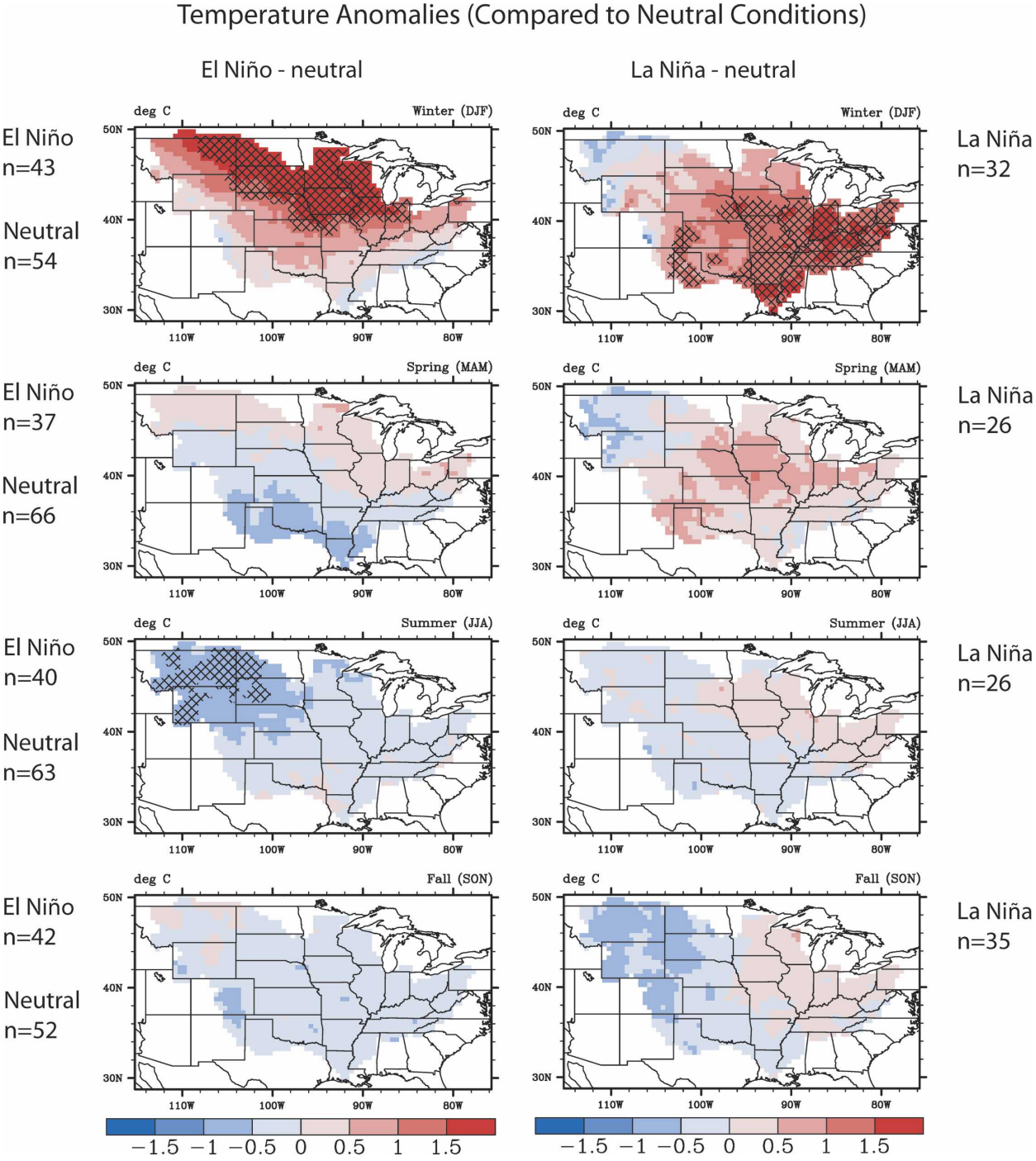

FIG. 3. Seasonal temperature anomalies (°C) compared to neutral conditions for El Niño and La Niña events, according to the CRU05 dataset (1958–2000). Differences significant at $p < 0.10$ are hatched, and degrees of freedom are given as the total numbers of months within each season.

to the northwest in summer but then disappear in fall when positive precipitation anomalies close to 1 mm day^{-1} are found in the northern tip and southern tier of the basin.

The general patterns of regional climate anomalies in the CRU05 data analysis agree with analyses of different datasets (Mason and Goddard 2001; Montroy et al. 1998; Smith et al. 1998), and with the anomaly patterns

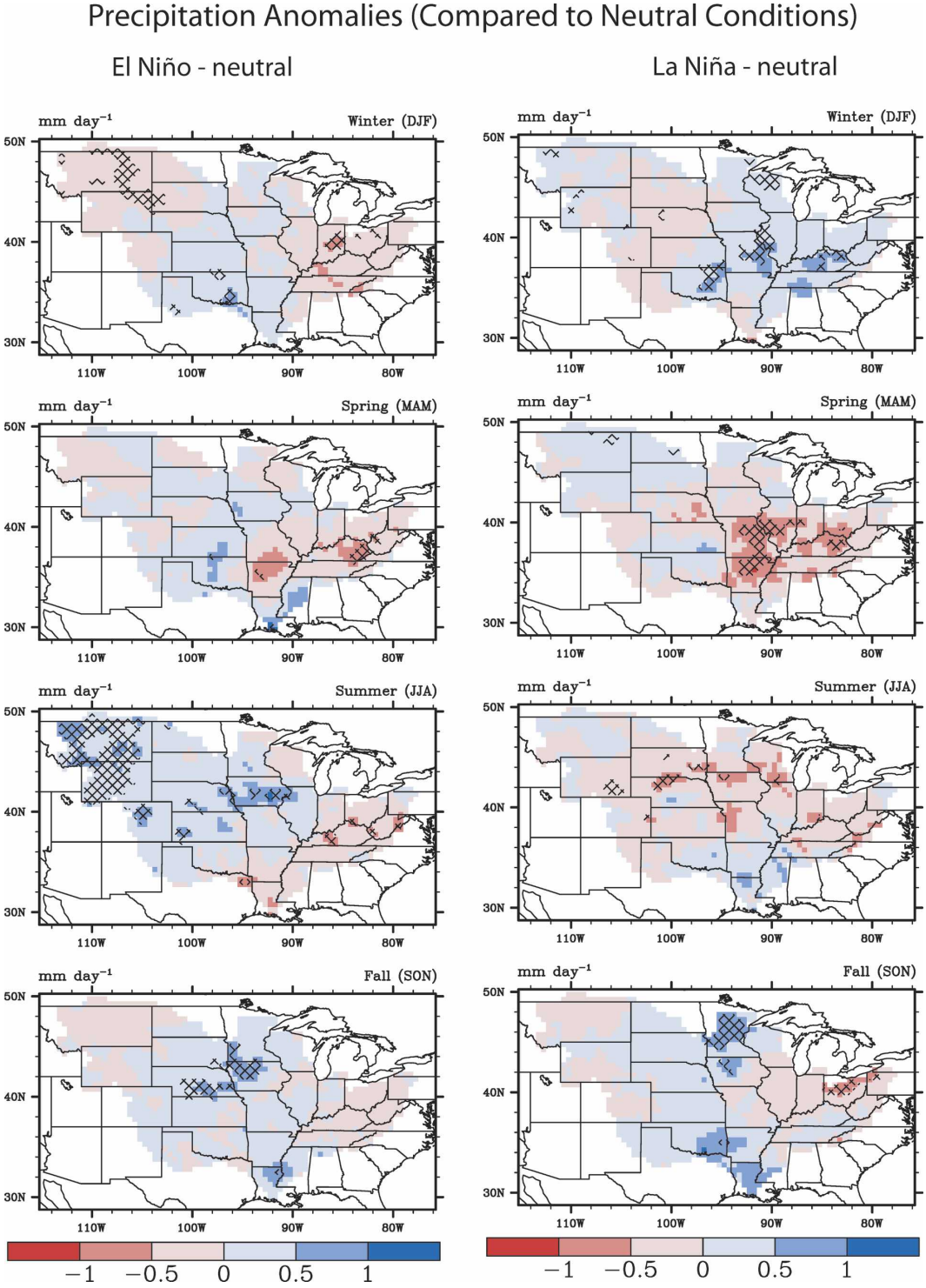

FIG. 4. Same as in Fig. 3, but for precipitation anomalies.

reported by the National Weather Service Climate Prediction Center (http://www.cpc.noaa.gov/products/precip/CWlink/ENSO/total.html#precip.click). These precipitation patterns highlight the diverse climatic conditions across the Mississippi River basin and illustrate that precipitation anomalies vary by location and season with no general pattern associated with either El Niño or La Niña.

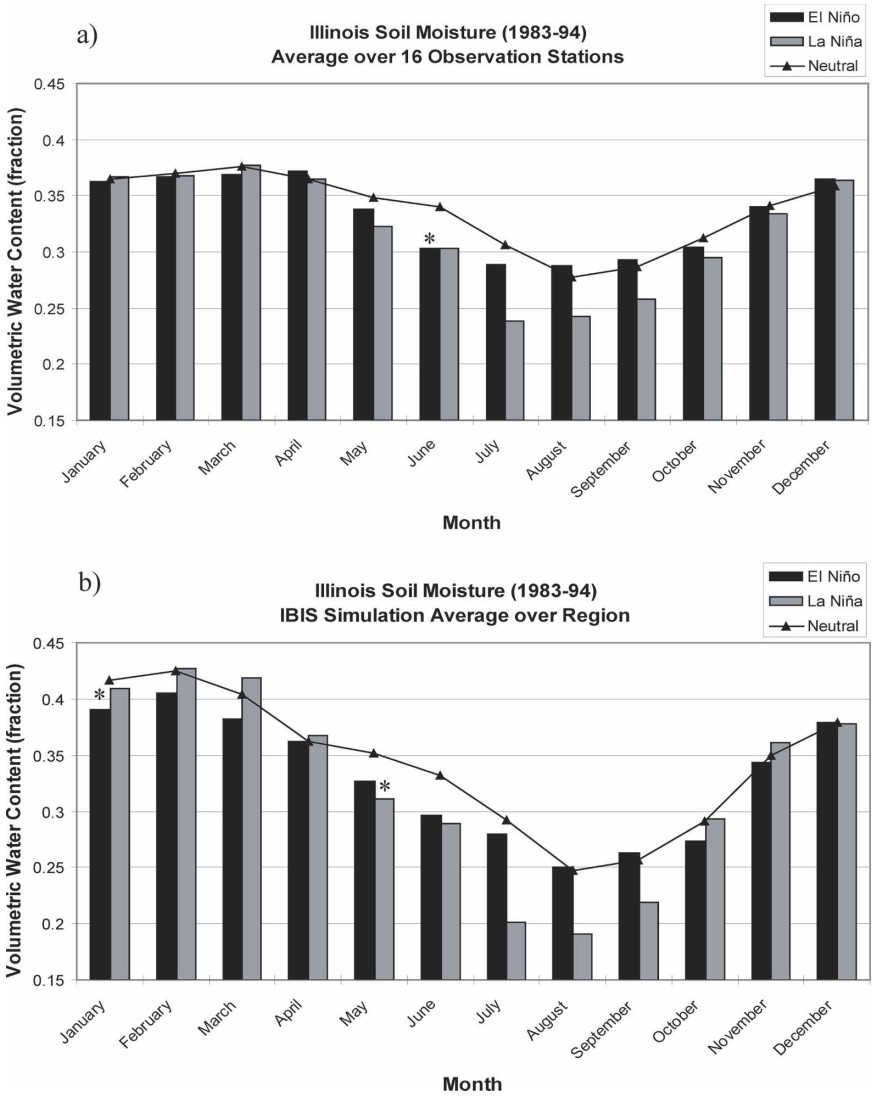

FIG. 5. Monthly soil moisture (in terms of volumetric water content) during neutral, El Niño, and La Niña conditions (a) averaged from observations from the 16 Illinois stations and (b) averaged over the region containing the stations as simulated by IBIS–HYDRA. The asterisk denotes months and events for which the difference from neutral conditions is statistically significant at $p < 0.10$.

4. Evaluation of ENSO: Simulation and observations

a. Soil moisture

The regional-averaged simulated soil moisture compares well with the observations both in magnitude and seasonal variability during neutral, El Niño, and La Niña months (Fig. 5). The month of maximum soil moisture occurs one month early in the model but the month of minimum simulated soil moisture (August) agrees with observations. Average monthly soil moisture is overestimated in winter by an average of 0.03 in the model, while values are underestimated by an average of 0.02 in April–October.

Only 5 El Niño and 2 La Niña events (an event is defined as consecutive months with one event type) occurred during the 1983–95 period of available soil moisture observations over Illinois, compared with the 13 El Niño and 8 La Niña events that occurred over the 43-yr period of our study. The five El Niño events are associated with negative anomalies in monthly average values of Illinois soil moisture during May, June, and

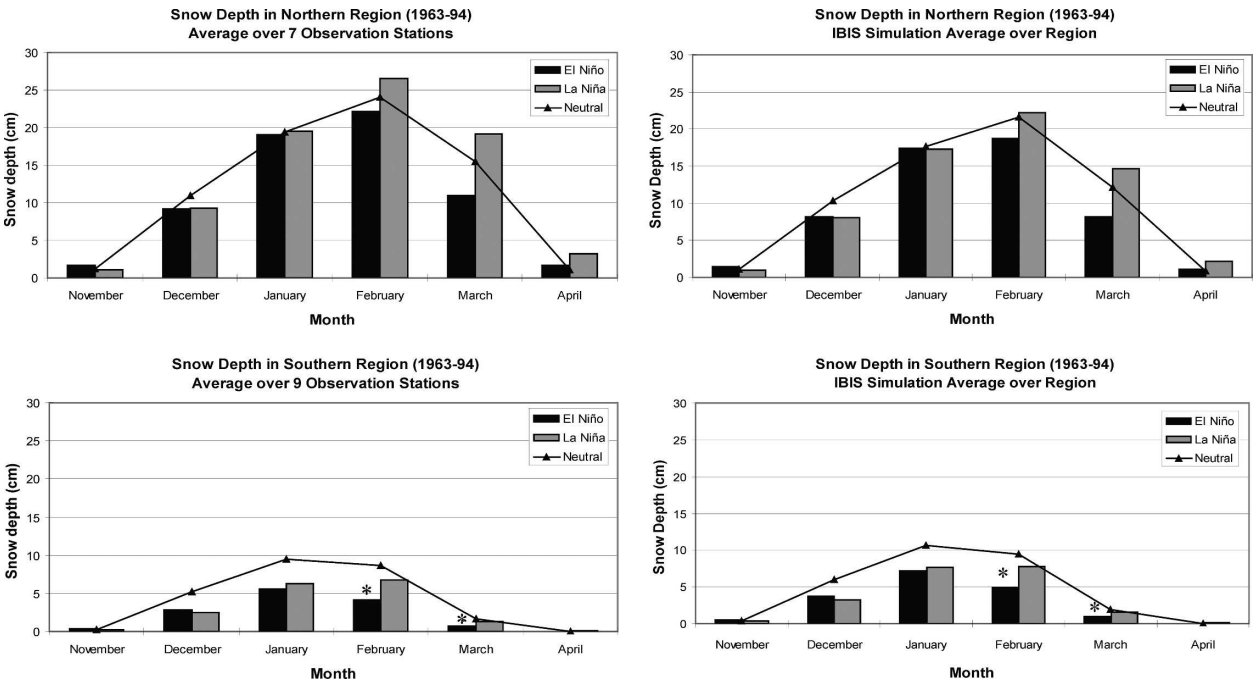

FIG. 6. Monthly winter snow depth (cm) during neutral, El Niño, and La Niña conditions (left) averaged from observations at 16 stations throughout the Midwest and (right) averaged over the regions containing the stations as simulated by IBIS–HYDRA. The asterisk denotes months and events for which the difference from neutral conditions is statistically significant at $p < 0.10$.

July, with the largest (0.04 or 12%) occurring in June (Fig. 5). Observed winter soil moisture during El Niño events shows no change from neutral years, while the model simulates negative anomalies. Both the observations and the model results show negative anomalies during El Niño summers and almost no anomaly throughout the fall season.

La Niña summers are also associated with negative Illinois soil moisture anomalies, although the anomalies are greater than during El Niño events and continue into fall (Fig. 5). Simulated values are underestimated during July–September by an average of 0.04 compared with observations. The model deviates slightly from the anomaly pattern seen in the observations in October, November, and March.

b. Snow depth

El Niño and La Niña may also affect the snow depth in snow-covered regions in terms of the amount of precipitation that falls as snow and the length of time snow remains. The NWS snow depth record covers most of the ENSO events because there were only neutral months from 1958 until 1963 when the snow data begin, although the record does not include the strong El Niño of 1997/98 and La Niña of 1998–2000.

In the northern region, the November–April average monthly snow depth from the NWS observations over the 192-month record is 12.0 cm during neutral events. The observed average snow depth decreases to 10.8 cm in El Niño winters and increases to 13.2 cm in La Niña winters. Maximum snow depth occurs in February in the north regardless of ENSO phase (Fig. 6). The negative anomaly in average El Niño snow depth is a result of negative anomalies during February and March, while the positive anomaly of average La Niña snow depth is largely the result of increased February, March, and April snow depth.

In the southern region, the November–April average snow depth from the NWS observations is 4.2 cm during neutral events. The observed average snow depth decreases during both El Niño and La Niña winters to 2.6 and 2.9 cm, respectively. The month of maximum snow depth in the south shifts from January in neutral and El Niño winters to a shared maximum in January and February in La Niña winters (Fig. 6).

IBIS captures the neutral average snow depth in the southern region with a November–April average value of 4.7 cm, while the northern region snow depth is underestimated by 2 cm. The month of maximum snow depth and patterns of change with ENSO are well simulated.

c. Streamflow

1) UPPER MISSISSIPPI SUBBASIN

According to the USGS data, positive anomalies of spring streamflow occur during El Niño in the Upper Mississippi throughout most of the year (Fig. 7), with the largest increase of 1266 $m^3 s^{-1}$ in April ($p < 0.13$). This pattern agrees with results of the Kahya and Dracup (1993) analysis in this region. The negative summer and fall streamflow anomalies during La Niña (of over 450 $m^3 s^{-1}$) are also consistent with the analysis of Dracup and Kahya (1994).

In general, the IBIS–HYDRA results of streamflow variations associated with ENSO agree with USGS streamgauge measurements (Fig. 7), although the USGS spring peak is delayed in the IBIS–HYDRA results.

2) OHIO SUBBASIN

The USGS streamflow measurements at Metropolis show negative anomalies during El Niño events throughout winter, spring, and summer (Fig. 7). Except for January and February, negative anomalies also occur throughout the year during La Niña events. The general patterns of change associated with ENSO are well-simulated by IBIS–HYDRA in the Ohio, although spring peak streamflow is underestimated by ~10% and is delayed by 1 month.

3) MISSOURI SUBBASIN

The largest changes to streamflow in the Missouri occur in April and May during La Niña events when there are negative anomalies of over 1000 $m^3 s^{-1}$ ($p < 0.07$; Fig. 7). While the model captures the positive anomalies during El Niño winter and negative anomalies during La Niña spring, the simulation results overestimate streamflow throughout the year, compared with the USGS measurements, because the model does not account for water regulation.

4) ARKANSAS SUBBASIN

Positive winter streamflow anomalies occur in the Arkansas during both El Niño and La Niña events (Fig. 7), according to the USGS data. The largest differences occur in February and March for both USGS and HYDRA datasets. These increases reach 1000 $m^3 s^{-1}$ (USGS; $p < 0.18$) and 945 $m^3 s^{-1}$ (HYDRA; $p < 0.13$) during La Niña events in March. Positive winter anomalies are followed by negative anomalies in spring and summer during both ENSO phases.

The seasonal pattern of streamflow change is reasonably captured in the model results. The spring peak is spread over a longer time period than is found in the observations, but the magnitude is simulated correctly. The August–September low flow period is slightly overestimated in the models, probably as a result of the neglect of water management.

5) WHOLE MISSISSIPPI BASIN

Streamflow at the outlet of the Mississippi River basin at Vicksburg is integrated from the outlets of the preceding subbasins; therefore, the magnitude is large and anomalies are diminished relative to upstream anomalies. There is little change to streamflow during El Niño events throughout the year (Fig. 7), although the positive winter La Niña anomalies from upstream basins, along with positive anomalies in the Lower Mississippi (not shown), contribute to positive USGS winter anomalies at Vicksburg (up to 5000 $m^3 s^{-1}$ in March; $p < 0.14$). Conversely, the negative La Niña anomalies in April and May propagate from upstream subbasins leading to a negative La Niña USGS anomaly in May of 5175 $m^3 s^{-1}$ ($p < 0.13$).

In general, HYDRA results compare well with the observations at Vicksburg, except in summer when streamflow is overestimated (up to 50% in July) as a result of overestimations within the Upper Mississippi, Missouri, and Arkansas (Fig. 7). The overall signals from El Niño and La Niña at Vicksburg are damped because of the variability in the upstream subbasins; therefore we conclude that there is no statistically significant association between either El Niño or La Niña and total Mississippi River basin streamflow. However, our results suggest that there are signals in upstream basins that vary by location and season. These results agree with those of other analyses (Dracup and Kahya 1994; Guetter and Georgakakos 1996; Kahya and Dracup 1993) and suggest that there are corresponding signals in surface water budget components. We discuss anomalies in these components in the following section.

5. ENSO and simulated surface water budget

Here we first describe the average water balance of neutral conditions, and then we describe the water balance anomalies associated with El Niño and La Niña events.

a. Average water balance in neutral conditions

Evapotranspiration is minimal across the Mississippi River basin in winter (Fig. 8). During spring, ET rates are largest over the warm and humid southeastern region of the basin as temperature and solar radiation

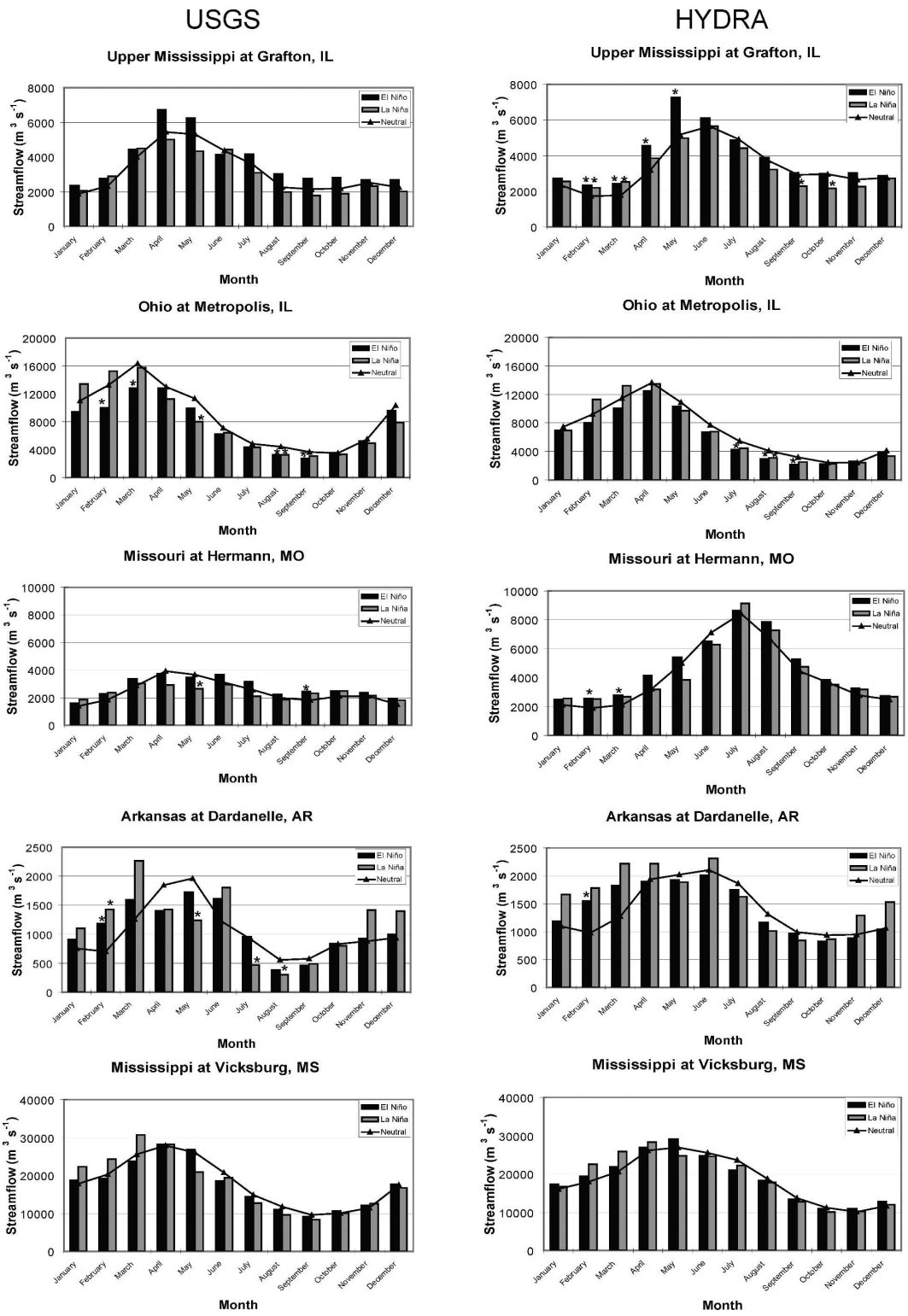

FIG. 7. Monthly streamflow ($m^3 s^{-1}$) during neutral, El Niño, and La Niña conditions at the outlets of the subbasins and the entire Mississippi basin as (left) estimated by USGS and (right) simulated by IBIS–HYDRA. The asterisk denotes months and events for which the difference from neutral conditions is statistically significant at $p < 0.10$.

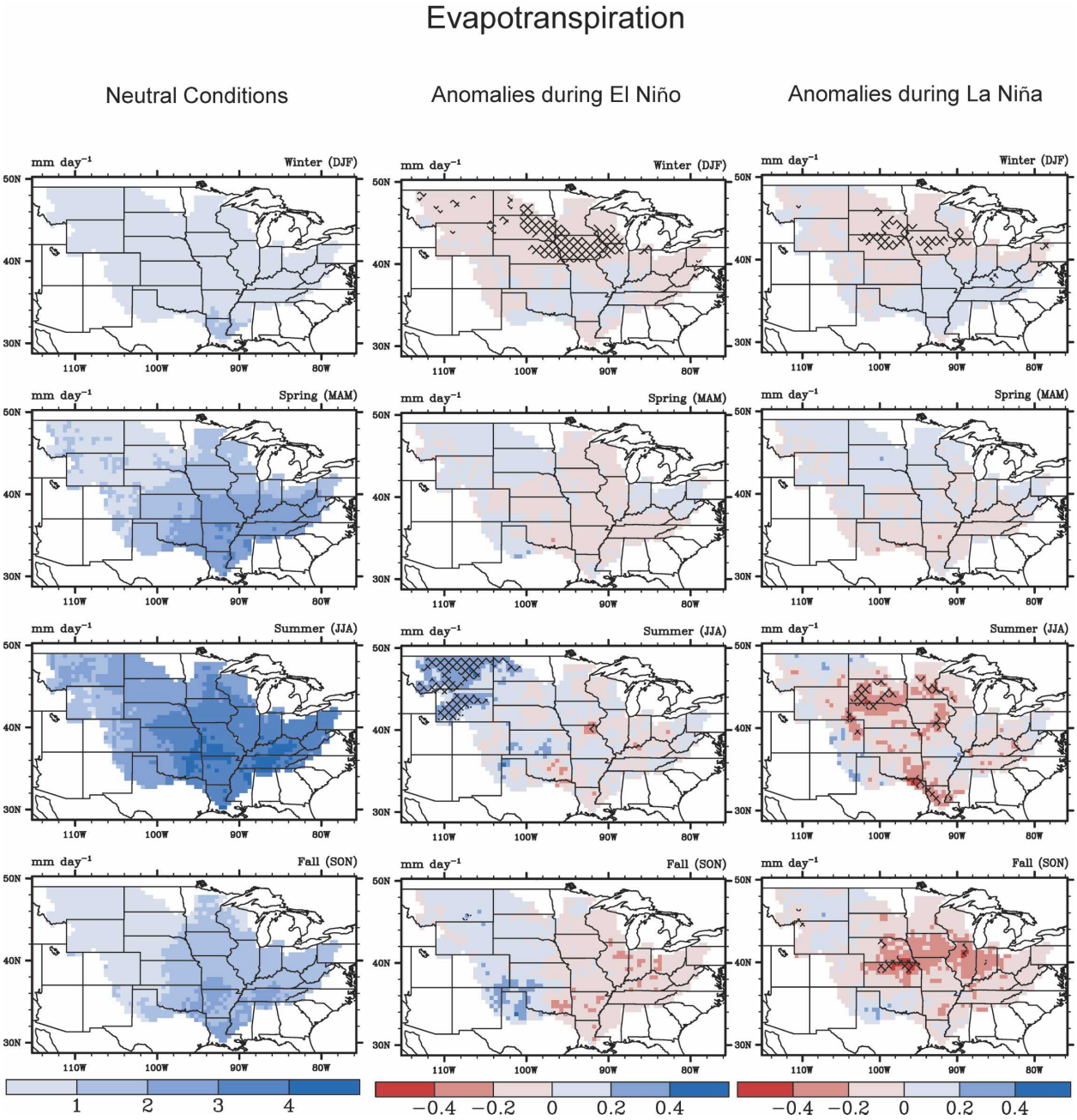

FIG. 8. Seasonal evapotranspiration (mm day^{-1}) during neutral conditions and anomalies compared to neutral conditions for El Niño and La Niña events, as simulated by IBIS–HYDRA for 1958–2000. Differences significant at $p < 0.10$ are hatched, and the degrees of freedom for each season are the same as shown in Fig. 3.

increase. By summer, ET rates are at maximum values across the basin (on average, between 3 and 4 mm day^{-1} in the south-central region and east, and about 2 mm day^{-1} in the west), but rates decrease rapidly by fall.

Soil moisture (defined as the fraction volumetric water content of the top 30 cm) tends to be greater in the humid, eastern half of the basin, and less in the drier, western half of the basin, although soil moisture varies throughout the year across the entire basin (Fig. 9). Maximum values (near 0.5, where 1.0 is saturated) are found during winter and spring. Evapotranspiration releases much of this stored water in summer such that summer and fall values of soil moisture are lower than winter and spring amounts.

Like soil moisture, total runoff is low in the drier,

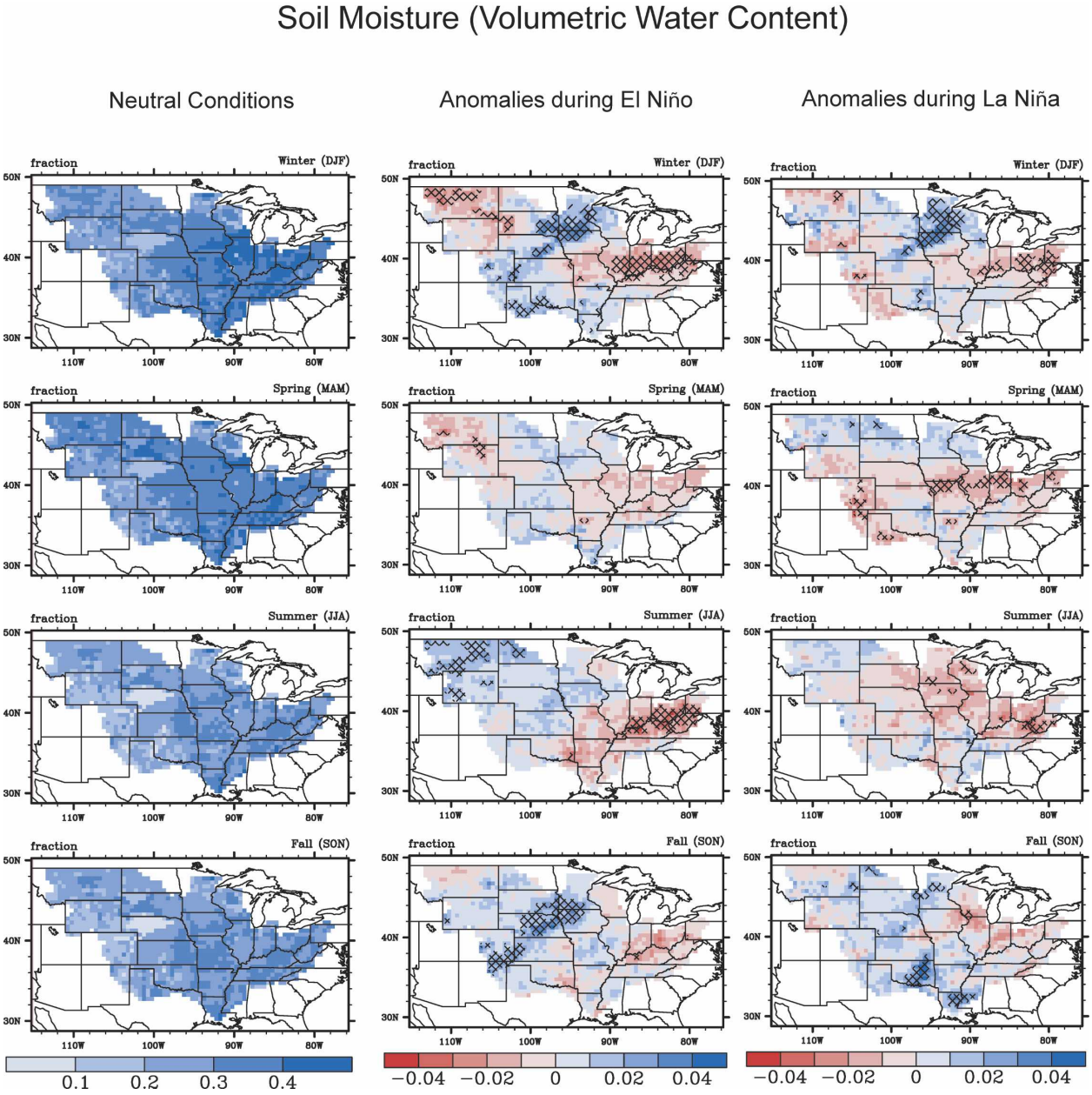

FIG. 9. Same as in Fig. 8, but for soil moisture (in terms of volumetric water content in the top 30 cm of soil).

western half of the basin (generally less than 1 mm day^{-1}) and can be more than 2 mm day^{-1} in the humid, eastern half of the basin where soil moisture seasonal variability is greater (Fig. 10). Total runoff is large in winter in the mountainous area of the eastern border and in the south where soil remains unfrozen in all seasons. Snowmelt causes maximum values of total runoff in spring throughout the central and eastern portions of the basin and in summer across the northern tier.

The average November–April snow depth during neutral winters increases from <2 cm northward from about the middle of the basin to just over 11 cm in northern Minnesota and Wisconsin and at the western mountainous border (Fig. 11).

b. El Niño and changes in the water balance

Precipitation anomalies associated with El Niño appear to force different responses in the western, central, and eastern portions of the basin. In the northwestern Missouri and Arkansas basins, positive summer precipitation anomalies lead to positive anomalies of

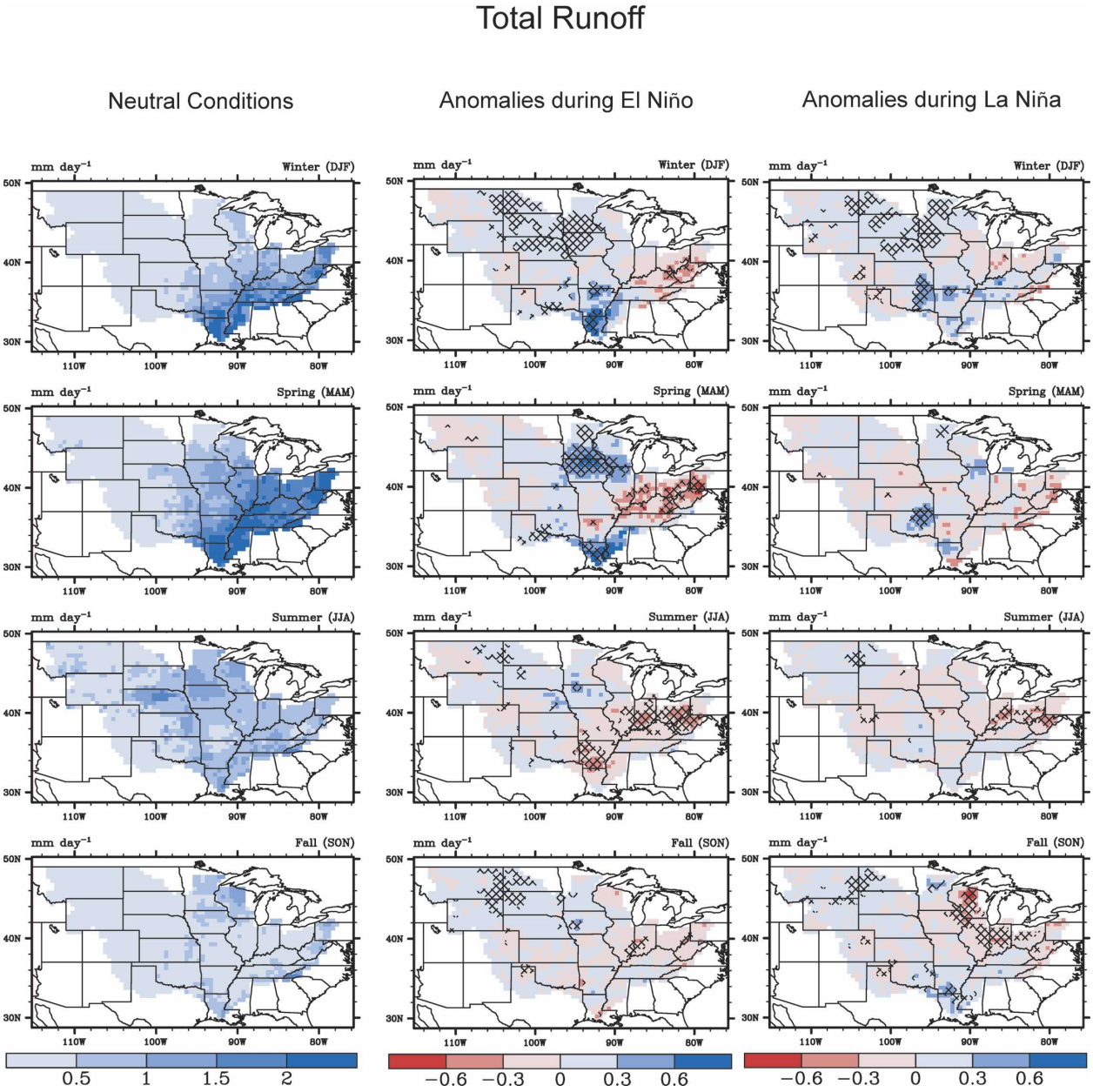

FIG. 10. Same as in Fig. 8, but for total runoff (sum of surface runoff and subsurface drainage).

ET in summer (Fig. 8), and soil moisture in summer and fall (Fig. 9), while having little effect on total runoff (Fig. 10).

Unlike the western half of the basin, precipitation anomalies in the central and southern portions of the basin mainly affect total runoff instead of ET. Positive precipitation anomalies through much of the Upper Mississippi and eastern Missouri basins in summer and fall, as well as positive anomalies in the southern tip in fall and winter (Fig. 4) cause positive anomalies of fall and winter soil moisture (Fig. 9) that lead to positive winter and spring runoff anomalies (over 0.6 mm day^{-1} or 50% in Iowa in spring; Fig. 10) with little effect on ET (Fig. 8). These positive runoff anomalies lead to the increases in Upper Mississippi spring streamflow (Fig. 7).

Precipitation anomalies mainly influence total runoff instead of ET in the eastern portion of the basin as well, but here the anomalies are negative. The scattered areas of negative precipitation anomalies in the eastern half of the basin throughout the year (Fig. 4) lead to negative anomalies of soil moisture throughout the year

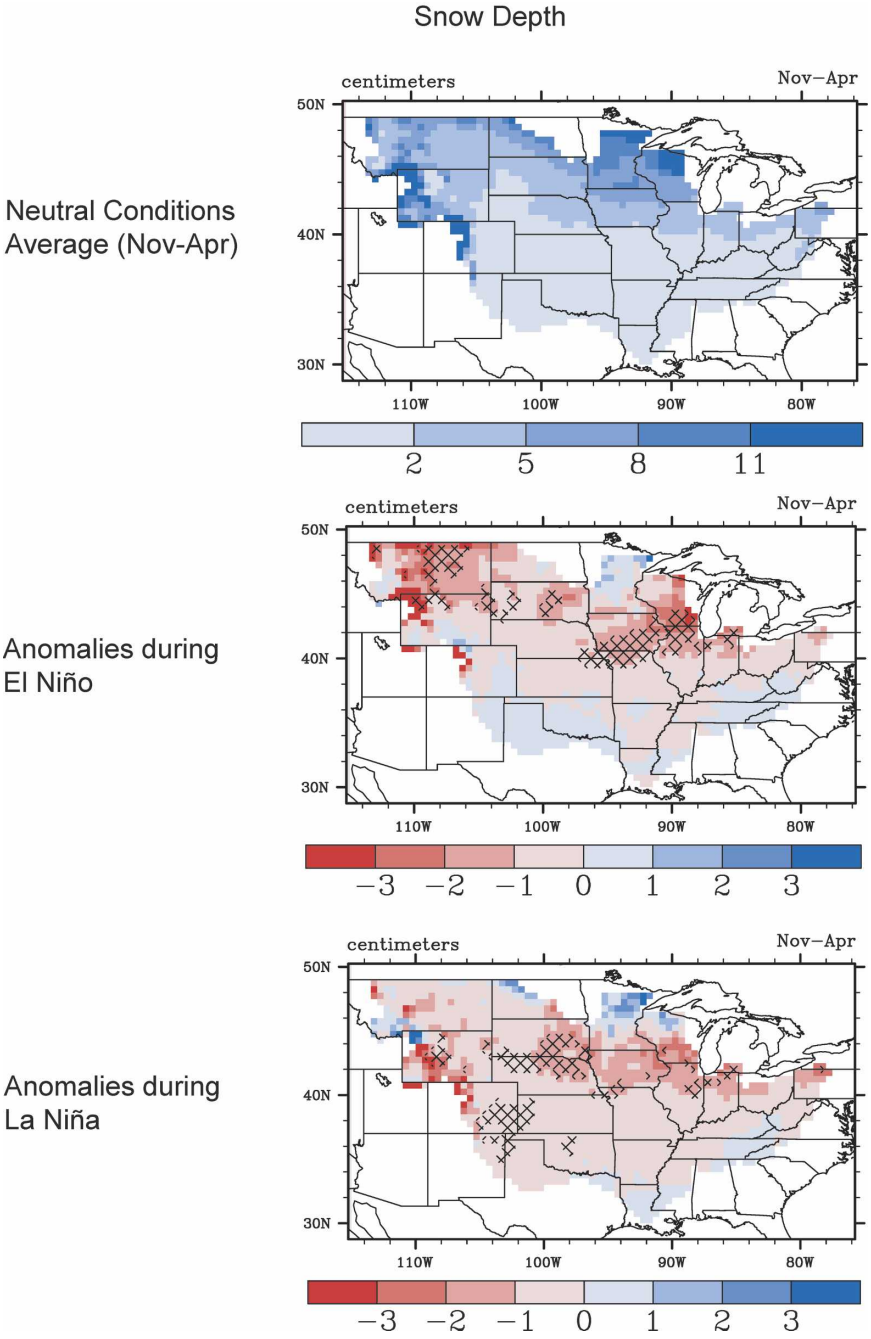

FIG. 11. Same as in Fig. 8, but for snow depth (cm).

(Fig. 9) that are consistent with spring and summer Illinois soil moisture observations (Fig. 5), large negative anomalies of total runoff (up to 0.5 mm day^{-1} or ~30%; Fig. 10) associated with negative streamflow anomalies in the Ohio subbasin (Fig. 7), and small (statistically insignificant) negative anomalies of ET (Fig. 8). Snow depth decreases by 35%–40% across the northern region during El Niño winters (Fig. 11). While not significant at $p < 0.10$, there is a region of increased snow depth in Minnesota that is consistent with the small region of increased snow depth in the Kunkel and Angel (1999) analysis.

A comparison of precipitation anomalies (Fig. 4) with anomalies of ET (Fig. 8), soil moisture (Fig. 9), and total runoff (Fig. 10) shows that widely scattered areas of precipitation anomalies (with little field signifi-

cance) can be associated with larger, coherent regions of soil moisture anomalies. These soil moisture anomalies then lead to ET anomalies in the west, or total runoff anomalies in the central and eastern subbasins. For example, the positive precipitation anomalies over the Central Plains in summer and fall lead to positive soil moisture anomalies that have a larger area of statistically significant differences in fall and winter. A similar pattern is seen in the Ohio subbasin where scattered negative precipitation anomalies throughout most of the year lead to a larger region of negative soil moisture anomalies.

These examples of small, scattered areas of precipitation anomalies that coalesce into larger regions of more significant soil moisture anomalies lend evidence to the idea of a terrestrial hydrologic memory in the land surface. This appears to describe a mechanism within the land surface that filters precipitation anomalies into larger, more significant anomalies of other water budget components in later seasons. While precipitation patterns generally follow synoptic-scale patterns that act at daily time scales, soil moisture anomalies reflect a seasonal response to seasonal climate anomalies. This mechanism is consistent with the ENSO simulation results of Chen and Kumar (2002).

c. La Niña and changes in the water balance

Negative precipitation anomalies in the Central Plains, Upper Mississippi, and Ohio basins during La Niña spring and summer (Fig. 4) lead to negative ET anomalies in summer and fall (up to 0.5 mm day^{-1} or ~15%; Fig. 8), negative anomalies in soil moisture (consistent with Illinois observations), and negative total runoff anomalies (Fig. 10). This contributes to negative streamflow anomalies in spring, summer, and fall from all upstream subbasins (Fig. 7).

Positive precipitation anomalies in the northern and southern tips of the basin in fall contribute to positive soil moisture anomalies in fall and winter, leading to increases in total runoff (over 0.6 mm day^{-1} or 20% in the south) because winter is a time of low ET. The positive winter precipitation anomalies in the Arkansas and southern Ohio subbasins lead to increased winter streamflow from the Ohio and Arkansas subbasins. As with the El Niño anomalies, the relatively noisy precipitation anomalies are integrated through the land surface into stronger areas of soil moisture anomalies in the south in fall and north in winter (Fig. 9).

Snow depth also decreases during La Niña winters in the Upper Mississippi region, although the negative anomalies are not as statistically significant as during El Niño winters. Snow depth increases in northern Minnesota and Wisconsin, despite positive temperature anomalies, as more simulated precipitation falls as snow and less as rain (results not shown). Although these increases are not statistically significant at $p < 0.10$, they agree with the analysis of Kunkel and Angel (1999). The decrease in snow depth during La Niña in the northern Ohio appears to be associated with positive temperature anomalies, as there is little change in total precipitation and snowfall. This result agrees with that of Serreze et al. (1998).

6. Variability of El Niño and La Niña responses

One question that results from the ENSO anomaly analysis is—how "typical" is the average El Niño/La Niña event? While the analyses in sections 3 through 5 show that both El Niño and La Niña are associated with different hydrologic anomalies in different portions of the Mississippi River basin, the use of a variable averaged over all El Niño/La Niña months does not quantify the variability of responses among all events. Statistically significant responses show a general pattern of anomalies that result with a particular ENSO phase, but outlying events may have significant impacts to society in terms of crop losses and flooding, for example.

A large amount of variability is illustrated through the difference in hydrologic variables between the weak El Niño event of 1969/70 and the strong El Niño event of 1997/98, and between the weak La Niña event of 1975/76 and the strong La Niña event of 1999/2000. For example, the 1997/98 winter precipitation in the Middle to Lower Mississippi and Arkansas region is 1–3 mm day^{-1} greater than the precipitation from 1969/70 (Fig. 12a), such that the difference in winter total runoff between the two winters (over 2.5 mm day^{-1} in Louisiana) is 4 times the difference between the average El Niño and neutral winters (Fig. 10). According to the USGS, winter streamflow from 1997/98 throughout the central, southern, and eastern portions of the basin was above average as a result of flooding in much of the south and along the South Platte and Ohio Rivers.

The greater than 6°C increase in winter temperature in 1999/98 in the Upper Mississippi compared with 1969/70 leads to November–April average snow depth that is 6–11 cm less in Minnesota and Wisconsin than the neutral average (Fig. 11). The average analysis of sections 3 through 5 shows no statistically significant change in snow depth during average El Niño winters in this region. Although there is little snow depth information from particularly strong El Niño events over the period of record, this analysis shows that a strong El Niño may have a much larger impact on snow cover in the northern Upper Mississippi basin than a typical El Niño winter, with ramifications for winter tourism and spring recharge from snowmelt events.

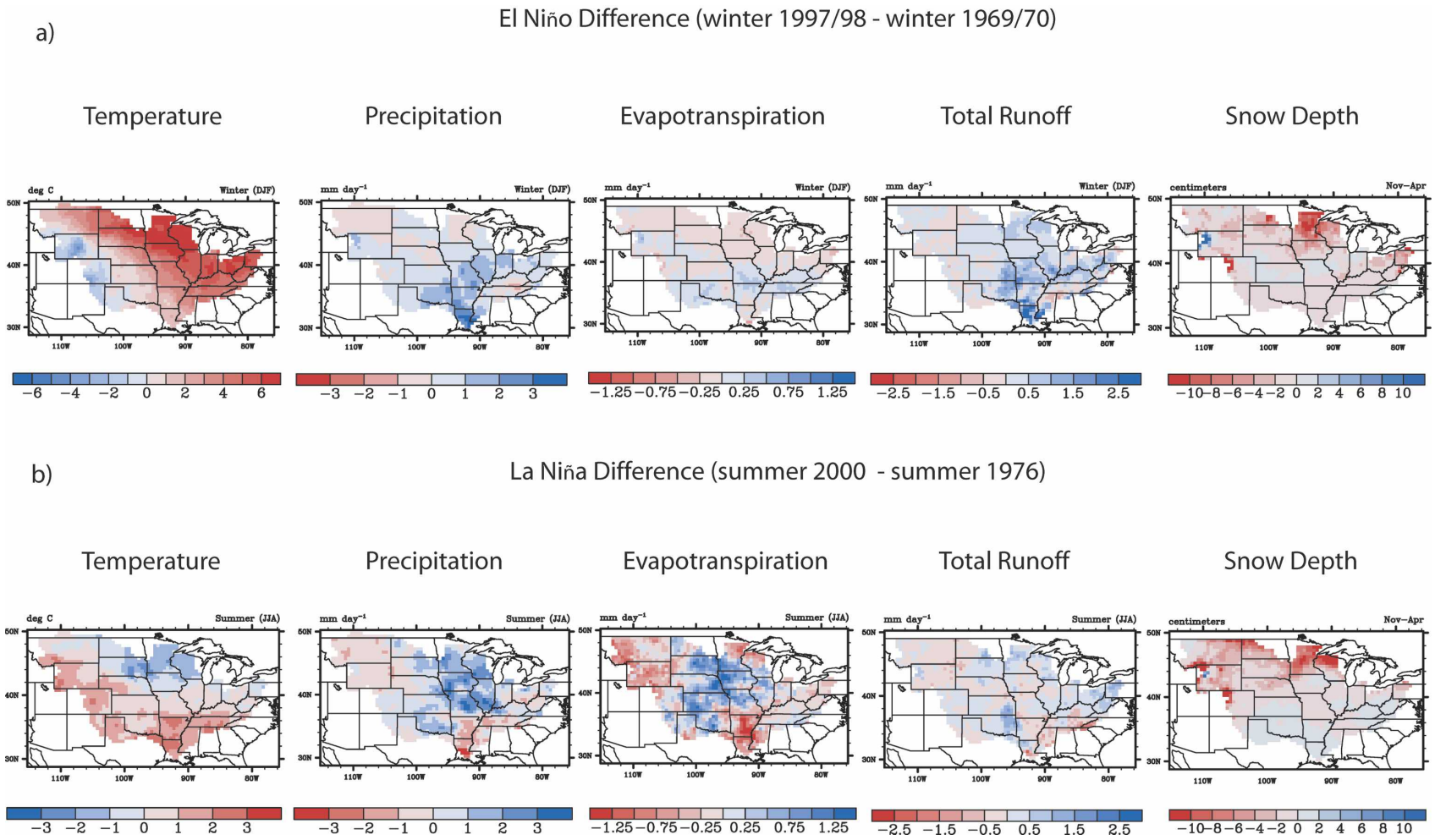

FIG. 12. (a) Differences of temperature and water balance components between the strong El Niño winter of 1997/98 and the weak El Niño winter of 1969/70, where weak is subtracted from strong, and (b) difference between the strong La Niña summer of 2000 and the weak La Niña summer of 1976. Note the change of scale between El Niño and La Niña temperature.

La Niña is associated with even greater variability among events. For example, the strong La Niña of 1999/2000 is associated with greater precipitation in the Arkansas basin in fall and winter (not shown), which reinforces the pattern seen from a typical La Niña (Fig. 4). However, precipitation during summer 2000 throughout the Midwest is up to 3 mm day^{-1} greater than precipitation from the summer of 1975 (Fig. 12b). This pattern contradicts the below-normal La Niña summer precipitation that occurs during a typical La Niña summer (Fig. 4). The large amount of summer 2000 precipitation produces simulated summer ET rates that are up to 1.5 mm day^{-1} greater than those simulated for the summer of 1976.

7. Summary and conclusions

The results of this study show that anomalous patterns of land surface hydrology within the Mississippi River basin are associated with El Niño and La Niña events, and that these patterns vary in time and space. While the analysis provides evidence of statistically significant anomalous patterns associated with typical El Niño and La Niña events, there is a large degree of variability in hydrologic response within each ENSO phase; however, the land surface can communicate precipitation anomalies, related to an ENSO event, across seasons and filter precipitation patterns into larger, more significant soil moisture anomalies.

Both phases of ENSO are associated with positive winter temperature anomalies, but precipitation anomalies alternate between positive and negative values depending on season, location, and ENSO phase. The increase in central and southern runoff and streamflow during El Niño is consistent with previous studies, although this study found increases in ET with little change in runoff in the western portion of the basin. One result not found in previous studies is a decrease in runoff and streamflow from the Ohio subbasin during El Niño events, but this region is geographically close to the northeast region of Kahya and Dracup (1993) in which negative anomalies of streamflow were found.

La Niña is typically associated with decreased ET in the central portion of the basin in summer and fall, decreased total runoff in the eastern portion, and increased total runoff during most of the year in the southern portion of the basin. These increases in runoff act to increase winter streamflow from the Ohio and the Arkansas, leading to increased streamflow at Vicksburg. While La Niña is associated with decreases in snow depth, similar to the response from El Niño, a small region of increased snow depth was simulated in northern Minnesota and Wisconsin, consistent with the results of a previous observational analysis (Kunkel and Angel 1999).

While this study highlights statistically significant responses to both ENSO phases during certain seasons and at specific locations, the analysis shows that there is a high degree of variability in response among El Niño and La Niña events—in some cases the response is several times larger than the average response. While it is important to understand a typical response to ENSO, a better understanding of extreme responses may lead to better preparation for a strong ENSO event. For example, the El Niño of 1982/83 is estimated to have caused \$10–\$12 billion in crop losses from drought (Wilhite et al. 1987). In addition, the prediction of large positive anomalies in ET, such as those simulated during the strong La Niña summer of 2000, may have implications for land–atmosphere feedbacks and recycling of moisture within the basin (Brubaker et al. 2001; Dirmeyer and Brubaker 1999; Findell and Eltahir 1997, 1999; Sudradjat et al. 2003; Zangvil et al. 2004).

The modeling system involved in this study provides a tool for further examination of land surface response to climate variability. A favorable comparison of IBIS–HYDRA results with the few available observations shows that the modeling system can reasonably simulate soil moisture, snow depth, and streamflow. This suggests that the modeling system can reasonably simulate water budget components for which we have few observations. The uncertainty in simulated streamflow is an accumulation of uncertainty in precipitation, soil moisture, and runoff and is similar to the current state of land surface process model simulation of streamflow (Lohmann et al. 2004). Despite some error in streamflow simulation, we believe the modeling system can still be used to "fill in" gaps in the observations (e.g., total runoff and ET) and to improve our understanding of the physical processes that cause ENSO-related responses in hydroclimatic variables. Future work should address the effects of other modes of climatic variability, as well as the hydrologic effects of interactions between ENSO and other anomalous climate patterns. Ultimately, a more complete understanding of how climatic variability affects regional hydrological processes may lead to improved understanding of how the basin operates and how it might respond to future environmental changes.

Acknowledgments. This research was funded through the NASA Land Surface Hydrology Program and the University of Wisconsin Graduate School, and was partially supported by a grant through the Office of Biological and Environmental Research Program (OBER), U.S. Department of Energy, through the

South Central Regional Center of the National Institute for Global Environmental Change (NIGEC) under Cooperative Agreement DE-FC03-90ER61010. The authors thank Michael Coe and Simon Donner for their help in directing the study and for their modeling expertise, John Lenters for providing soil moisture and snow depth data, and two anonymous reviewers whose suggestions greatly enhanced the content and presentation of this study.

REFERENCES

Berbery, E., Y. Luo, K. Mitchell, and A. Betts, 2003: Eta model estimated land surface processes and the hydrologic cycle of the Mississippi basin. *J. Geophys. Res.,* **108,** 8852, doi:10.1029/2002JD003192.

Betts, A., J. Ball, M. Bosilovich, P. Viterbo, Y. Zhang, and W. Rossow, 2003: Intercomparison of water and energy budgets for five Mississippi subbasins between ECMWF reanalysis (ERA-40) and NASA Data Assimilation Office fvGCM for 1990–1999. *J. Geophys. Res.,* **108,** 8618, doi:10.1029/2002JD003127.

Brubaker, K. L., P. A. Dirmeyer, A. Sudradjat, B. S. Levy, and F. Bernal, 2001: A 36-yr climatological description of the evaporative sources of warm-season precipitation in the Mississippi River basin. *J. Hydrometeor.,* **2,** 537–557.

Campbell, G. S., and J. M. Norman, 1998: *An Introduction to Environmental Biophysics*. Springer-Verlag, 286 pp.

Chen, J., and P. Kumar, 2002: Role of terrestrial hydrologic memory in modulating ENSO impacts in North America. *J. Climate,* **15,** 3569–3585.

Coe, M. T., 2000: Modeling terrestrial hydrological systems at the continental scale: Testing the accuracy of an atmospheric GCM. *J. Climate,* **13,** 686–704.

——, and J. A. Foley, 2001: Human and natural impacts on the water resources of the Lake Chad basin. *J. Geophys. Res.,* **106,** 3349–3356.

——, M. H. Costa, A. Botta, and C. Birkett, 2002: Long-term simulations of discharge and floods in the Amazon basin. *J. Geophys. Res.,* **107,** 8044, doi:10.1029/2001JD000740.

Costa, M. H., and J. A. Foley, 1997: Water balance of the Amazon Basin: Dependence on vegetation cover and canopy conductance. *J. Geophys. Res.,* **102,** 23 973–23 989.

Delire, C., and J. A. Foley, 1999: Evaluating the performance of a land surface/ecosystem model with biophysical measurements from contrasting environments. *J. Geophys. Res.,* **104,** 16 895–16 909.

Dirmeyer, P., and K. Brubaker, 1999: Contrasting evaporative moisture sources during the drought of 1988 and the flood of 1993. *J. Geophys. Res.,* **104,** 19 383–19 397.

Donner, S. D., 2003: The impact of cropland cover on river nutrient levels in the Mississippi River Basin. *Global Ecol. Biogeogr.,* **12,** 341–355.

——, and C. J. Kucharik, 2003: Evaluating the impacts of land management and climate variability on crop production and nitrate export across the Upper Mississippi Basin. *Global Biogeochem. Cycles,* **17,** 1085, doi:10.1029/2001GB001808.

——, M. T. Coe, J. D. Lenters, T. E. Twine, and J. A. Foley, 2002: Modeling the impact of hydrological changes on nitrate transport in the Mississippi River Basin from 1955 to 1994. *Global Biogeochem. Cycles,* **16,** 1043, doi:10.1029/2001GB001396.

Dracup, J. A., and E. Kahya, 1994: The relationships between U.S. streamflow and La Niña events. *Water Resour. Res.,* **30,** 2133–2141.

Findell, K. L., and E. A. B. Eltahir, 1997: An analysis of the soil moisture-rainfall feedback, based on direct observations from Illinois. *Water Resour. Res.,* **33,** 725–735.

——, and ——, 1999: Analysis of the pathways relating soil moisture and subsequent rainfall in Illinois. *J. Geophys. Res.,* **104,** 31 565–31 574.

Foley, J. A., I. C. Prentice, N. Ramankutty, S. Levis, D. Pollard, S. Sitch, and A. Haxeltine, 1996: An integrated biosphere model of land surface processes, terrestrial carbon balance, and vegetation dynamics. *Global Biogeochem. Cycles,* **10,** 603–628.

——, A. Botta, and M. T. Coe, 2002: El Niño–Southern oscillation and the climate, ecosystems and rivers of Amazonia. *Global Biogeochem. Cycles,* **16,** 1132, doi:10.1029/2002GB001872.

Gershunov, A., and T. P. Barnett, 1998: Interdecadal modulation of ENSO teleconnections. *Bull. Amer. Meteor. Soc.,* **79,** 2715–2725.

Goolsby, D. A., and Coauthors, 1999: Flux and sources of nutrients in the Mississippi-Atchafalaya River basin: Topic 3 Report for the Integrated Assessment on Hypoxia in the Gulf of Mexico. NOAA Coastal Ocean Office, Series No. 17, 130 pp.

Guetter, A., and K. Georgakakos, 1996: Are the El Niño and La Niña predictors of the Iowa River seasonal flow? *J. Appl. Meteor.,* **35,** 690–705.

Hollinger, S. E., and S. A. Isard, 1994: A soil moisture climatology of Illinois. *J. Climate,* **7,** 822–833.

Kahya, E., and J. A. Dracup, 1993: U.S. streamflow patterns in relation to the El Niño/Southern Oscillation. *Water Resour. Res.,* **29,** 2491–2503.

Kalnay, E., and Coauthors, 1996: The NCEP/NCAR 40-Year Reanalysis Project. *Bull. Amer. Meteor. Soc.,* **77,** 437–471.

Kistler, R., and Coauthors, 2001: The NCEP–NCAR 50-year reanalysis: Monthly means CD-ROM and documentation. *Bull. Amer. Meteor. Soc.,* **82,** 247–268.

Kucharik, C. J., 2003: Evaluation of a process-based agro-ecosystem model (Agro-IBIS) across the U.S. cornbelt: Simulations of the interannual variability in maize yield. *Earth Interactions,* **7**. [Available online at http://EarthInteractions.org.]

——, and Coauthors, 2000: Testing the performance of a Dynamic Global Ecosystem Model: Water balance, carbon balance, and vegetation structure. *Global Biogeochem. Cycles,* **14,** 795–825.

——, K. R. Brye, J. M. Norman, J. A. Foley, S. T. Gower, and L. G. Bundy, 2001: Measurements and modeling of carbon and nitrogen cycling in agroecosystems of southern Wisconsin: Potential for SOC sequestration during the next 50 years. *Ecosystems,* **4,** 237–258.

Kunkel, K. E., and J. R. Angel, 1999: Relationship of ENSO to snowfall and related cyclone activity in the contiguous United States. *J. Geophys. Res.,* **104,** 19 425–19 434.

Lenters, J. D., M. T. Coe, and J. A. Foley, 2000: Surface water balance of the continental United States, 1963–1995: Regional evaluation of a terrestrial biosphere model and the NCEP/NCAR reanalysis. *J. Geophys. Res.,* **105,** 22 393–22 425.

Lohmann, D., and Coauthors, 2004: Streamflow and water balance intercomparisons of four land surface models in the North American Land Data Assimilation System project. *J. Geophys. Res.,* **109,** D07S91, doi:10.1029/2003JD003517.

Mason, S. J., and L. Goddard, 2001: Probabilistic precipitation

anomalies associated with ENSO. *Bull. Amer. Meteor. Soc.,* **82,** 619–638.

Maurer, E. P., and D. P. Lettenmaier, 2003: Predictability of seasonal runoff in the Mississippi River basin. *J. Geophys. Res.,* **108,** 8607, doi:10.1029/2002JD002555.

Miller, D. A., and R. A. White, 1998: A conterminous United States multilayer soil characteristics dataset for regional climate and hydrology modeling. *Earth Interactions,* **2**. [Available online at http://EarthInteractions.org.]

Montroy, D. L., M. B. Richman, and P. J. Lamb, 1998: Observed nonlinearities of monthly teleconnections between tropical Pacific sea surface temperature anomalies and central and eastern North American precipitation. *J. Climate,* **11,** 1812–1835.

New, M., M. Hulme, and P. D. Jones, 1999: Representing twentieth-century space–time climate variability. Part I: Development of a 1961–90 mean monthly terrestrial climatology. *J. Climate,* **12,** 829–856.

——, ——, and ——, 2000: Representing twentieth-century space–time climate variability. Part II: Development of 1901–96 monthly grids of terrestrial surface climate. *J. Climate,* **13,** 2217–2238.

Ramankutty, N., and J. A. Foley, 1998: Characterizing patterns of global land use: An analysis of global croplands data. *Global Biogeochem. Cycles,* **12,** 667–685.

——, and ——, 1999: Estimating historical changes in land cover: North American crops from 1850 to 1992. *Global Ecol. Biogeogr.,* **8,** 381–396.

Roads, J., and Coauthors, 2003: GCIP water and energy budget synthesis (WEBS). *J. Geophys. Res.,* **108,** 8609, doi:10.1029/2002JD002583.

Robock, A., 2003: Preface to special section: GEWEX Continental-Scale International Project (GCIP)-3. *J. Geophys. Res.,* **108,** 8605, doi:10.1029/2003JD003924.

Ropelewski, C. F., and M. S. Halpert, 1986: North American precipitation and temperature patterns associated with the El Niño/Southern Oscillation (ENSO). *Mon. Wea. Rev.,* **114,** 2352–2362.

Serreze, M. C., M. P. Clark, D. L. McGinnis, and D. A. Robinson, 1998: Characteristics of snowfall over the eastern half of the United States and relationships with principal modes of low-frequency atmospheric variability. *J. Climate,* **11,** 234–250.

Smith, S. R., P. M. Green, A. P. Leonardi, and J. J. O'Brien, 1998: Role of multiple-level tropospheric circulations in forcing ENSO winter precipitation anomalies. *Mon. Wea. Rev.,* **126,** 3102–3116.

Sudradjat, A., K. Brubaker, and P. Dirmeyer, 2003: Interannual variability of surface evaporative moisture sources of warm-season precipitation in the Mississippi River basin. *J. Geophys. Res.,* **108,** 8612, doi:10.1029/2002JD003061.

Thompson, S. L., and D. Pollard, 1995a: A global climate model (GENESIS) with a land-surface transfer scheme (LSX). Part I: Present climate simulation. *J. Climate,* **8,** 732–761.

——, and ——, 1995b: A global climate model (GENESIS) with a land-surface transfer scheme (LSX). Part II: CO_2 sensitivity. *J. Climate,* **8,** 1104–1121.

Trenberth, K. E., 1997: The definition of El Niño. *Bull. Amer. Meteor. Soc.,* **78,** 2771–2777.

Twine, T., C. Kucharik, and J. Foley, 2004: Effects of land cover change on the energy and water balance of the Mississippi River basin. *J. Hydrometeor.,* **5,** 640–655.

Wilhite, D. A., D. A. Wood, and S. J. Meyer, 1987: Climate-related impacts in the United States during the 1982–83 El Niño. *Climate Crisis*, M. Glantz, R. Katz, and M. Krenz, Eds., UNEP, 75–78.

Zangvil, A., D. Portis, and P. Lamb, 2004: Investigation of the large-scale atmospheric moisture field over the midwestern United States in relation to summer precipitation. Part II: Recycling of local evapotranspiration and association with soil moisture and crop yields. *J. Climate,* **17,** 3283–3301.